

Terahertz atmospheric attenuation and continuum effects

David M. Slocum,^{*a} Thomas M. Goyette,^a Elizabeth J. Slingerland,^{†a} Robert H. Giles,^a and William E. Nixon^b

^aSubmillimeter-Wave Technology Laboratory, University of Massachusetts Lowell, Lowell, MA 01854, United States; ^bUnited States Army, National Ground Intelligence Center, Charlottesville, VA 22911, United States

ABSTRACT

Remote sensing over long path lengths has become of greater interest in the terahertz frequency region. Applications such as pollution monitoring and detection of energetic chemicals are of particular interest. Although there has been much attention to atmospheric effects over narrow frequency windows, accurate measurements across a wide spectrum is lacking. The water vapor continuum absorption spectrum was investigated using Fourier Transform Spectroscopy. The continuum effect gives rise to an excess absorption that is unaccounted for in just a resonant line spectrum simulation. The transmission of broadband terahertz radiation from 0.300THz - 1.5THz through air with varying relative humidity levels was recorded for multiple path lengths. From these data, the absorption coefficient as a function of frequency was determined and compared with model calculations. The intensity and location of the strong absorption lines were in good agreement with spectral databases such as the 2008 HITRAN database and the JPL database. However, a noticeable continuum effect was observed particularly in the atmospheric transmission windows. A small discrepancy still remained even after accounting for continuum absorption using the best available data from the literature. This discrepancy, when projected over a one kilometer path length, typical of distances used in remote sensing, can cause a 30dB difference between calculated and observed attenuation. From the experimental and resonant line simulation spectra the air-broadening continuum parameter was calculated and compared with values available in the literature.

Keywords: water vapor; atmospheric absorption; continuum; terahertz; spectroscopy

1 INTRODUCTION

The propagation of electromagnetic radiation, in particular at terahertz frequencies, through the Earth's atmosphere is an important field of study. Applications like remote sensing, imaging, detection of concealed items, astronomical observations, and more are used in industries like defense, medical, environmental, and academia and are more commonly employing terahertz frequencies. Water vapor has thousands of rotational and vibrational absorption lines positioned throughout the whole electromagnetic spectrum and is a main contributor to atmospheric attenuation in the terahertz regime. Propagation of radiation over extended distances is not feasible at many frequencies. Measurements to be performed in this frequency region require significant attention to the specific environment.

The absorption peaks of water vapor have been extensively studied¹⁻³ however the window regions between the strong absorption lines are more difficult to characterize. Current models⁴⁻⁸ require the use of an empirical continuum contribution to the spectrum for an accurate comparison to experimental spectra. In the microwave region there is much evidence that the continuum contribution scales as the square of the frequency with a negative dependence on temperature.⁸⁻¹⁰ However, at higher frequencies in the terahertz region only a few studies have seen the quadratic dependence on frequency.¹¹⁻¹³ Further complicating the issue, there is uncertainty as to the cause of the continuum as well as the values of the continuum parameters. Since the continuum contribution is empirical, it depends on both experimental data as well as model predictions. The choice of line parameters, line shape function, and number of

* Corresponding author. Email: David_Slocum@student.uml.edu phone: 978-934-1300 www.stl.uml.edu

† Current address: Metron Inc., 1818 Library St Ste 600, Reston, VA 20190, United States

Report Documentation Page				Form Approved OMB No. 0704-0188	
Public reporting burden for the collection of information is estimated to average 1 hour per response, including the time for reviewing instructions, searching existing data sources, gathering and maintaining the data needed, and completing and reviewing the collection of information. Send comments regarding this burden estimate or any other aspect of this collection of information, including suggestions for reducing this burden, to Washington Headquarters Services, Directorate for Information Operations and Reports, 1215 Jefferson Davis Highway, Suite 1204, Arlington VA 22202-4302. Respondents should be aware that notwithstanding any other provision of law, no person shall be subject to a penalty for failing to comply with a collection of information if it does not display a currently valid OMB control number.					
1. REPORT DATE MAY 2013		2. REPORT TYPE		3. DATES COVERED 00-00-2013 to 00-00-2013	
4. TITLE AND SUBTITLE Terahertz atmospheric attenuation and continuum effects				5a. CONTRACT NUMBER	
				5b. GRANT NUMBER	
				5c. PROGRAM ELEMENT NUMBER	
6. AUTHOR(S)				5d. PROJECT NUMBER	
				5e. TASK NUMBER	
				5f. WORK UNIT NUMBER	
7. PERFORMING ORGANIZATION NAME(S) AND ADDRESS(ES) University of Massachusetts Lowell,Submillimeter-Wave Technology Laboratory,Lowell,MA,01854				8. PERFORMING ORGANIZATION REPORT NUMBER	
9. SPONSORING/MONITORING AGENCY NAME(S) AND ADDRESS(ES)				10. SPONSOR/MONITOR'S ACRONYM(S)	
				11. SPONSOR/MONITOR'S REPORT NUMBER(S)	
12. DISTRIBUTION/AVAILABILITY STATEMENT Approved for public release; distribution unlimited					
13. SUPPLEMENTARY NOTES					
14. ABSTRACT Remote sensing over long path lengths has become of greater interest in the terahertz frequency region. Applications such as pollution monitoring and detection of energetic chemicals are of particular interest. Although there has been much attention to atmospheric effects over narrow frequency windows, accurate measurements across a wide spectrum is lacking. The water vapor continuum absorption spectrum was investigated using Fourier Transform Spectroscopy. The continuum effect gives rise to an excess absorption that is unaccounted for in just a resonant line spectrum simulation. The transmission of broadband terahertz radiation from 0.300THz - 1.5THz through air with varying relative humidity levels was recorded for multiple path lengths. From these data, the absorption coefficient as a function of frequency was determined and compared with model calculations. The intensity and location of the strong absorption lines were in good agreement with spectral databases such as the 2008 HITRAN database and the JPL database. However, a noticeable continuum effect was observed particularly in the atmospheric transmission windows. A small discrepancy still remained even after accounting for continuum absorption using the best available data from the literature. This discrepancy, when projected over a one kilometer path length, typical of distances used in remote sensing, can cause a 30dB difference between calculated and observed attenuation. From the experimental and resonant line simulation spectra the air-broadening continuum parameter was calculated and compared with values available in the literature.					
15. SUBJECT TERMS					
16. SECURITY CLASSIFICATION OF:			17. LIMITATION OF ABSTRACT Same as Report (SAR)	18. NUMBER OF PAGES 14	19a. NAME OF RESPONSIBLE PERSON
a. REPORT unclassified	b. ABSTRACT unclassified	c. THIS PAGE unclassified			

absorption lines used in the model can significantly affect the calculation of the continuum parameters. Also a limited number of experimental studies performed at terahertz frequencies restricts a comprehensive and accurate determination of the continuum parameters. Only a few broadband studies have been performed in the terahertz region, most of which were performed in a laboratory environment using either pure nitrogen or oxygen gas as the foreign broadening gas.¹²⁻¹⁵ Control over the experimental conditions is gained through the sacrifice of the broadening gas, which is of a different composition from Earth's atmosphere. Other works have studied atmospheric air,^{11,16-18} however these studies do not have control over many of the experimental parameters.

The present study used dry air as the foreign broadening gas, which has the same composition of atmospheric air, while maintaining control over the experimental parameters. Broadband transmission data was taken between 0.3-1.5THz over multiple path lengths and humidity levels to determine the absorption coefficient of atmospheric air. These results were combined with simulated absorption coefficient data calculated using line parameters from the 2008 HITRAN Database¹⁹ (HITRAN) to find the air-broadened continuum coefficient. When the continuum contribution is incorporated into the absorption coefficient calculations, the resulting spectrum can be used to identify the best frequency range for which an experiment is to be performed.

2 PROCEDURE

2.1 Experimental setup

Fourier Transform Spectroscopy (FTS) was used to collect transmission data of terahertz radiation through air with varying relative humidity levels and path lengths. A Pike Technologies variable path length gas cell was used to contain the sample and allow for multiple path length measurements. Figure 1 shows a schematic of the experimental setup along with a diagram of the variable path length gas cell. The cell was mounted into the sample chamber of a Bruker Vertex 80V Fourier Transform Infrared (FTIR) Spectrometer with a mercury arc lamp source aligned to the optical path of the spectrometer. The transmitted radiation was collected using a liquid helium cooled bolometer from IR labs with a vacuum pump attached to the liquid helium chamber to lower the operating temperature to 1.6K.

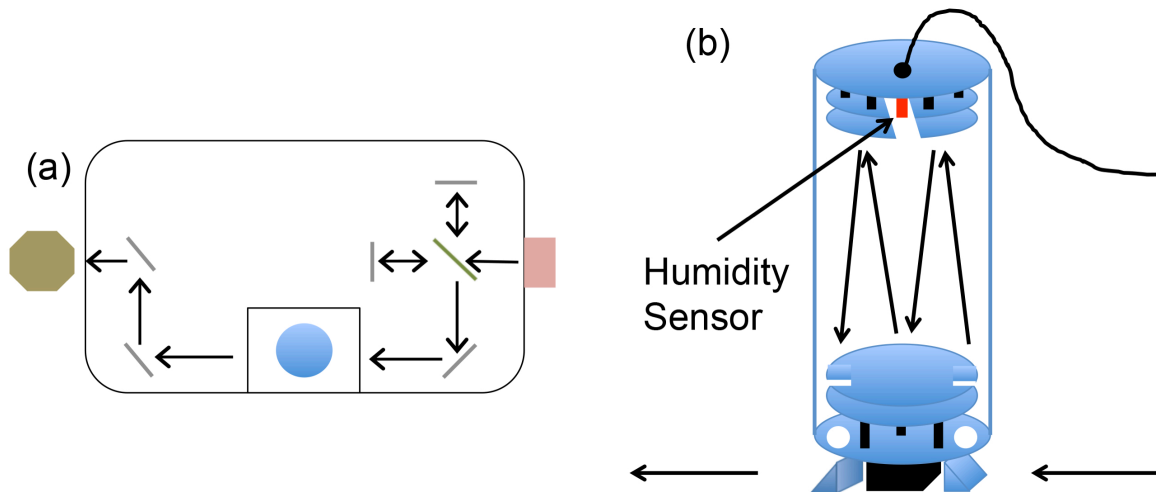


Figure 1. The FTIR with absorption cell in blue is shown in (a), while (b) shows the multipath absorption cell.

The variable path length cell used in the experiment was able to achieve 1-6m path lengths in 1m increments. The path length was adjusted through a micrometer screw on the top of the cell without the need to realign the setup. The cell was connected to a vacuum pump and sample containers. The pressure of the system was monitored using external capacitance manometers allowing for measurements from 0.01-1000Torr. In addition a Honeywell HIH-4000 humidity sensor was mounted in the cell, which allowed for an independent measure of the relative humidity, and hence the partial pressure of water vapor, inside the cell.

2.2 Transmission measurements and absorption coefficient calculations

Transmission data were recorded from 300-1500GHz with a resolution of 3GHz. The FTIR used a 125 μ m Mylar beamsplitter, which has a null at 720GHz. The bolometer also had a cold filter, which attenuated radiation above 1500GHz. As stated previously, each dataset had 6 transmission scans, one for each path length. A total of 4 relative humidity levels were studied, 17.89, 36.79, 48.03, and 70.84% relative humidity. These relative humidity levels correspond to 3.60, 8.04, 10.05, and 15.23Torr partial pressure of water vapor respectively at 296K.

To collect a transmission scan the cell was evacuated to below 10mTorr and sealed for background measurements. Background measurements were recorded for 1-6m path lengths consecutively. After the background scans were completed, distilled water vapor followed by dry air was introduced into the cell and then sealed. Sample scans for path lengths of 1-6m were then completed and normalized to the corresponding background scan.

The absorption coefficient was then calculated from the transmission data using the Beer-Lambert Law, $\tau = \exp(-\alpha l)$, where τ is the normalized transmission, α is the absorption coefficient, and l is the path length of the cell. The absorption coefficient is then found to be the slope of the straight line fit of the logarithm of the transmission versus the path length, as shown in Eq. (1).

$$\alpha l = -\ln(\tau) \quad (1)$$

3 ABSORPTION COEFFICIENT CALCULATIONS

A detailed description of the absorption coefficient calculations can be found elsewhere,²⁰ so only a brief description of the calculations will be given here. The calculations for an absorption coefficient spectrum were performed in five successive steps for direct comparison with experimental datasets.

Step one of the calculations is to simulate the self-broadened absorption line. The line parameters for each absorption line were obtained from HITRAN and were used in Eq.(2),the Van Vleck-Weisskopf line shape function.²¹

$$\alpha_k(\nu) = \alpha_{k,\max} \frac{\nu}{\nu_k} \left[\frac{1}{\left(\frac{\nu - \nu_k}{\Delta \nu_k} \right)^2 + 1} + \frac{1}{\left(\frac{\nu + \nu_k}{\Delta \nu_k} \right)^2 + 1} \right] \quad (2)$$

In Eq. (2), α_k and $\alpha_{k,\max}$ are the absorption coefficient of the k^{th} line in the database and the amplitude of the self broadened absorption line in units of m^{-1} and ν , ν_k , and $\Delta \nu_k$ are the frequency of the incident radiation, line center frequency, and line half width respectively in MHz.

Step two of the calculations is to account for the effects of foreign gas broadening. Equation (2) is again used to calculate the foreign gas broadened line shape. The whole line shape is then multiplied by a normalization factor so that the integrated line strength is the same as the self broadened line shape from step one. Figure 2 shows a comparison of the two pressure-broadened line shapes as well as a Doppler-broadened line shape. As can be seen in the figure, the effect of foreign gas broadening is to decrease the peak amplitude and increase the line width.

Step three is to take the sum of all of the foreign gas broadened absorption lines in the frequency region to produce the resonant line absorption coefficient spectrum. **Step four** is then to account for the continuum contribution to the absorption coefficient. The water vapor continuum can be accurately modeled by Eq. (3)^{8-10,13-14}

$$\alpha_c(\nu) = \nu^2 P_s \left(P_s C_s \theta^{n_s} + P_f C_f \theta^{n_f} \right) \quad (3)$$

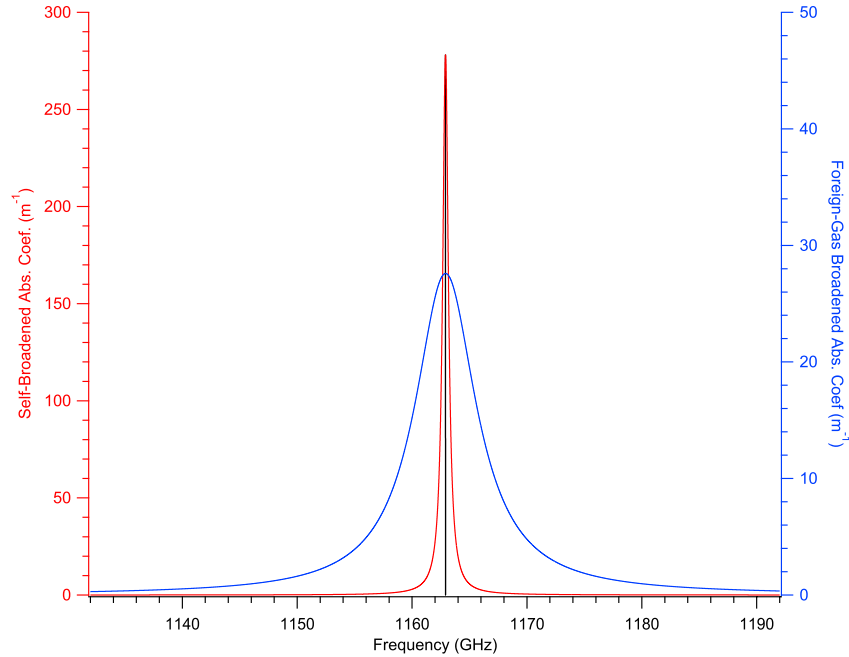


Figure 2. A Doppler-broadened absorption line with the partial pressure of water vapor equal to the critical pressure (black) and two pressure-broadened absorption lines; a self-broadened line with 15.23Torr of water vapor (red) and a foreign gas broadened line with 15.23Torr of water vapor and 746.77Torr of air (blue).

In Eq. (3), α_c is the continuum contribution to the absorption coefficient in units of m^{-1} , C_s and C_f are the self and foreign continuum coefficients in units of $\text{m}^{-1}/(\text{Torr}^2\text{MHz}^2)$, P_s and P_f are the sample and foreign gas pressures in units of Torr, the exponential terms n_s and n_f are the self and foreign temperature exponents, and θ is a reference temperature divided by the gas temperature in Kelvin.

The continuum component of the absorption coefficient, as calculated from Eq. (3), is then added to the resonant line absorption coefficient spectrum calculated in step three to produce the total absorption coefficient. **Step five** is to account for the instrumentation distortion of the experimental apparatus. The FTIR uses discrete resolution bins of finite width in the Fast Fourier Transform of the transmission spectra. This distortion is modeled by applying the same discrete resolution bins to the calculated spectra.

The effects of steps 3-5 and the resulting spectra can be seen in Figure 3. The continuum absorption has a small but measurable contribution to the total absorption coefficient. This contribution, however, is only significant in the transmission windows between the strong spectral lines. At the peaks of the strong spectral lines the continuum contribution to the absorption coefficient is unnoticeable. In the figure this can be clearly seen as a difference between the green and red spectra in the windows, while at the peaks the green and red spectra overlap each other and are indistinguishable. Also shown in the Figure 3 are the effects of the instrumentation distortion. The effect is to lower and broaden the spectral lines. The distortion is only significant in the strong spectral lines and is unnoticeable in the transmission windows because the absorption coefficient has a much smaller gradient in these regions. Again this can be clearly seen in the figure, however for the distortion the red and blue spectra overlap and are indistinguishable in the window regions and in the peaks there is a clear difference between the red and blue spectra.

It is necessary to account for any instrumentation distortion in the calculated spectrum to make an accurate comparison with the experimental peak amplitudes. The difference between the peak amplitudes of a calculated spectrum with and without instrumentation distortion for a resolution of 3GHz can be significant. If this distortion is unaccounted for direct comparison of calculated spectra and experimental spectra will yield poor results. This distortion also restricts the comparison of two experimental spectra directly without similar instrumentation distortion or adjustments to one or both of the spectra.

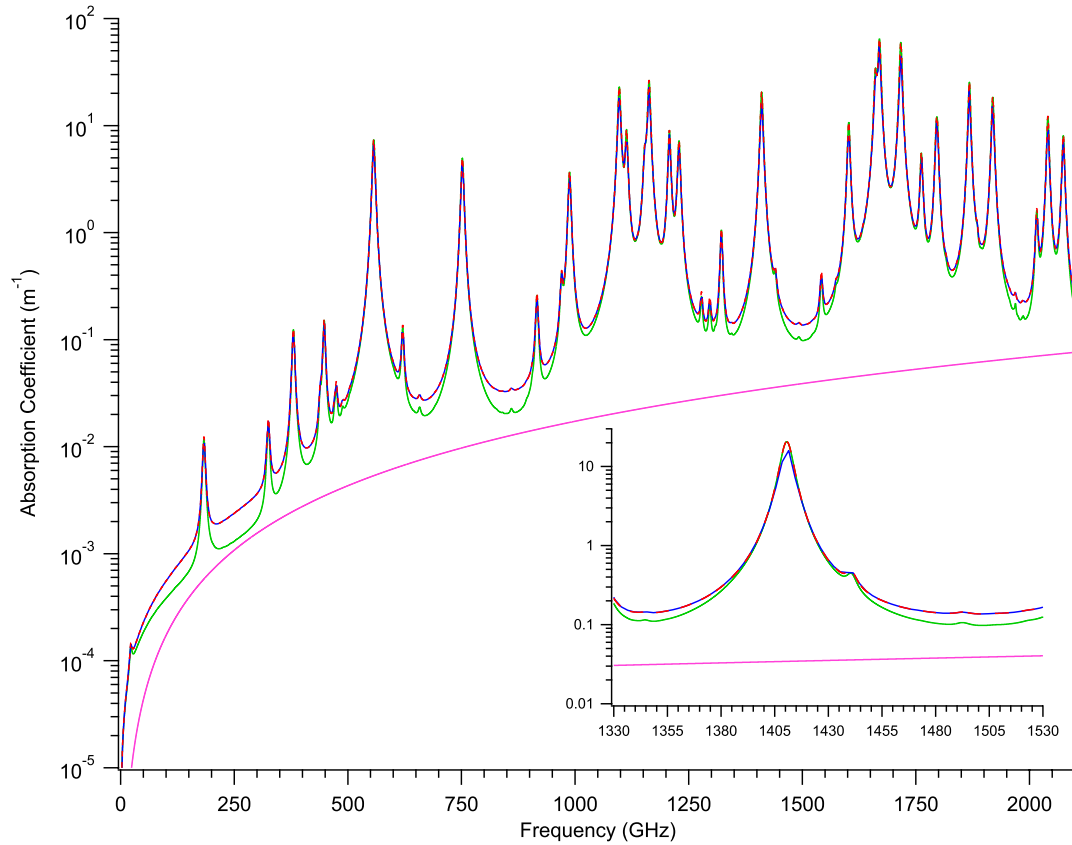


Figure 3. The results from the absorption coefficient calculations. The air-broadened spectrum (green), continuum absorption (pink), air-broadened spectrum with continuum absorption (dashed red), and air-broadened spectrum with continuum absorption and instrumentation distortion (blue). All plots are 15.23Torr of water vapor and 746.77Torr or air.

4 RESULTS

The transmission plots of 1-6m path lengths for terahertz radiation through air with relative humidity levels of 17.89, 36.78, 48.03, and 70.84% were recorded and the dataset for 70.84% relative humidity is shown in Figure 4. The width of the studied frequency region was limited by the power emitted from the source and a cold filter in the bolometer on the low and high end of the region. As seen in the figure, there is a region of significant noise centered at 720GHz, which is due to a beamsplitter null. Also seen in the figure are saturation effects in many of the strong absorption lines, particularly in the frequency range from 1.05-1.25THz.

The absorption coefficient was calculated for each dataset according to the process outline in Section 2.2 and is shown for 70.84% relative humidity in Figure 5. Slocum et al.²⁰ published the full results of the study including plots of all four datasets for the transmission and absorption coefficient. The effects of saturation can be seen in the strong absorption lines as regions of missing data. Saturation limited the calculation of the absorption coefficient to values less than 4m^{-1} . The statistical error for each data point was calculated from the fitting routine of the absorption coefficient. The average error across the data range, excluding regions of low signal to noise, was 8.85, 4.00, 3.67, and 2.87% for the 17.89, 36.78, 48.03, and 70.84% relative humidity datasets respectively.

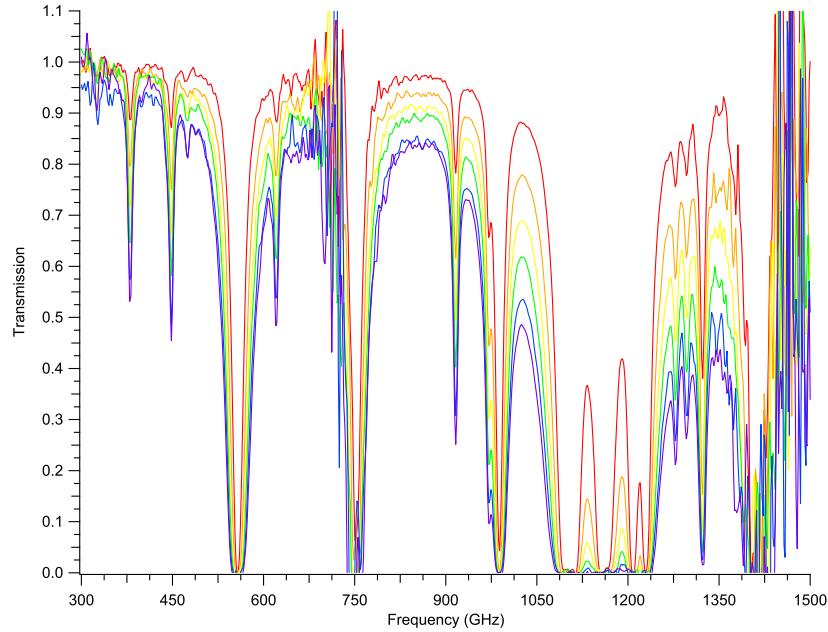


Figure 4. The experimental transmission of air with a relative humidity of 70.84% for 1-6m. The red, orange, yellow, green, blue, and purple plots correspond to 1-6m respectively.

The empirical continuum absorption data was found from taking the difference of the experimental absorption coefficient data and the calculated absorption coefficient data without compensating for continuum absorption. This was then used to determine the air-broadened continuum coefficient by fitting the continuum absorption to Eq. (3). The fitting parameter was $C_f^* = C_f \theta_f^n$ since all of the data from the present study were at a constant temperature of 296K so θ_f^n is a multiplicative constant for the present study. The value obtained of $C_f^* = 1.158 \times 10^{-18} \text{ m}^{-1}/(\text{Torr}^2 \text{ MHz}^2)$ was found to minimize the mean square error of the four datasets. The fitting routine employed the value of C_s^* from Podobedov et al.^{13,14} of $1.76 \times 10^{-17} \text{ m}^{-1}/(\text{Torr}^2 \text{ MHz}^2)$, which yielded a minimum for the mean square error when compared with other values from the literature.

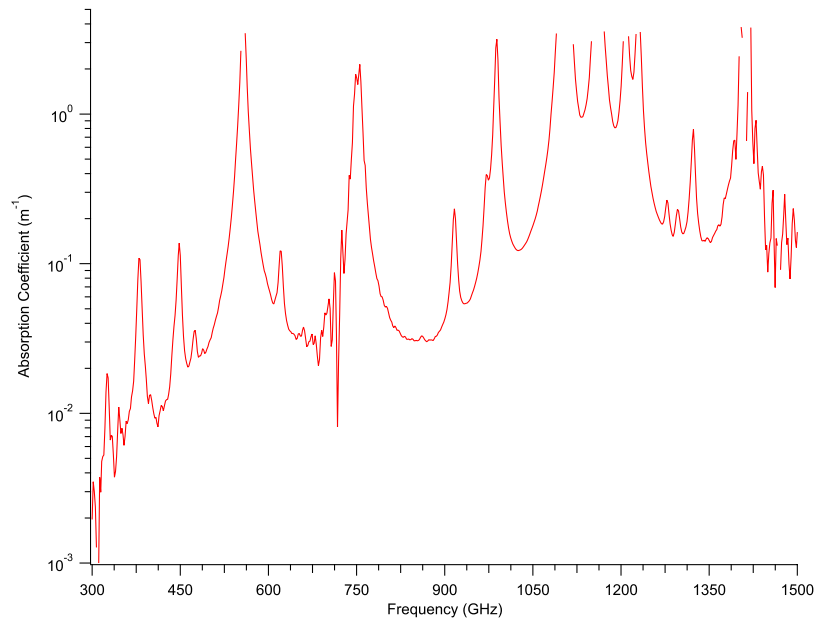


Figure 5. The experimentally determined absorption coefficient for air with a relative humidity of 70.84%.

5 ANALYSIS

The calculated and experimental absorption coefficients were converted from units of m^{-1} to dB/km in the remainder of the paper for ease of use[‡]. The experimental spectra were compared with calculated values from the process outlined in Section 3. The continuum contribution to the absorption coefficient was calculated using parameter sets from Kuhn et al.,⁹ Podobedov et al.,^{13,14} and the present study. The residual of each of these calculated spectra with the experimental spectra was a minimum for the continuum parameter set from the present study. The results of this comparison can be seen in Figure 6. Given these results, only the continuum parameter set from the present study is used for comparison to the experimental data. Figure 7 shows the calculated spectrum along with the experimental absorption coefficient spectrum. As can be seen, when the continuum is unaccounted for there are significant discrepancies between the experimental and calculated spectra in the window regions. However, after the continuum contribution has been added there is very good agreement between the experimental and calculated spectra. It can also be seen, as stated previously, that in the peaks of the spectra there is no noticeable difference between the two calculated spectra and the continuum absorption only makes a significant contribution in the window regions.

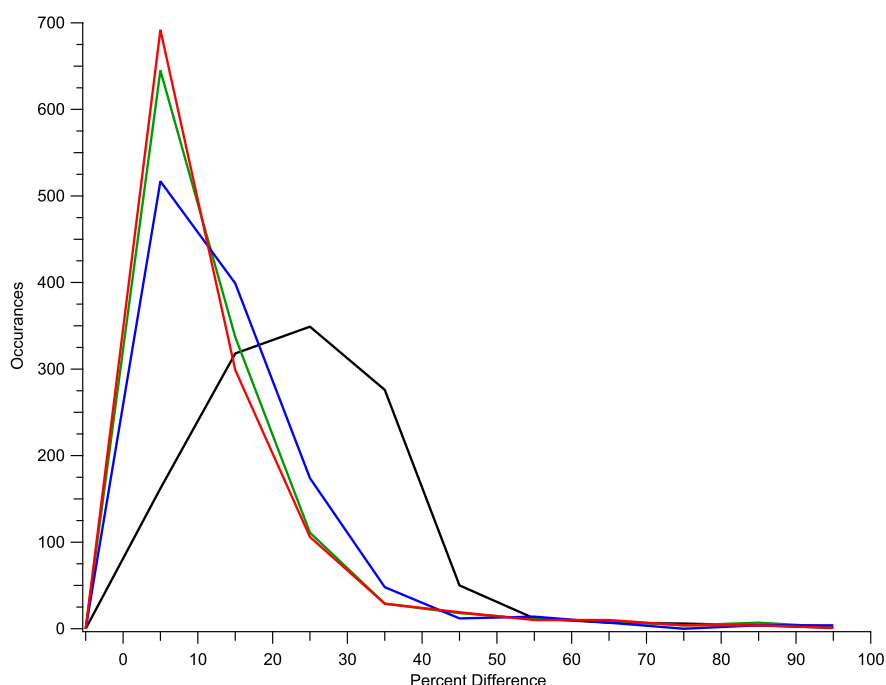


Figure 6. A histogram of the percent difference with a bin size of 10 points between the observed spectra and the calculated spectra using different continuum parameter sets. The plot shows comparisons with calculations using the continuum parameter set from the present study (red), Kuhn et al. (green), Podobedov et al. (blue) and with no continuum (black).

Figure 8 shows an expanded view of the atmospheric window at 870GHz. As discussed previously, the calculated spectrum without continuum effects does a poor job of reproducing the experimental spectrum. However, when continuum absorption is accounted for in the calculations there is good agreement between the calculated and experimental spectra. Also seen in the figure is an absorption peak located at 916GHz. It can be seen that for the absorption line it is not necessary to account for continuum absorption to yield an accurate comparison, both calculated spectra are in good agreement with the experimental spectrum at the absorption line.

[‡] $1\text{m}^{-1}=4.343\times 10^3\text{dB/km}$

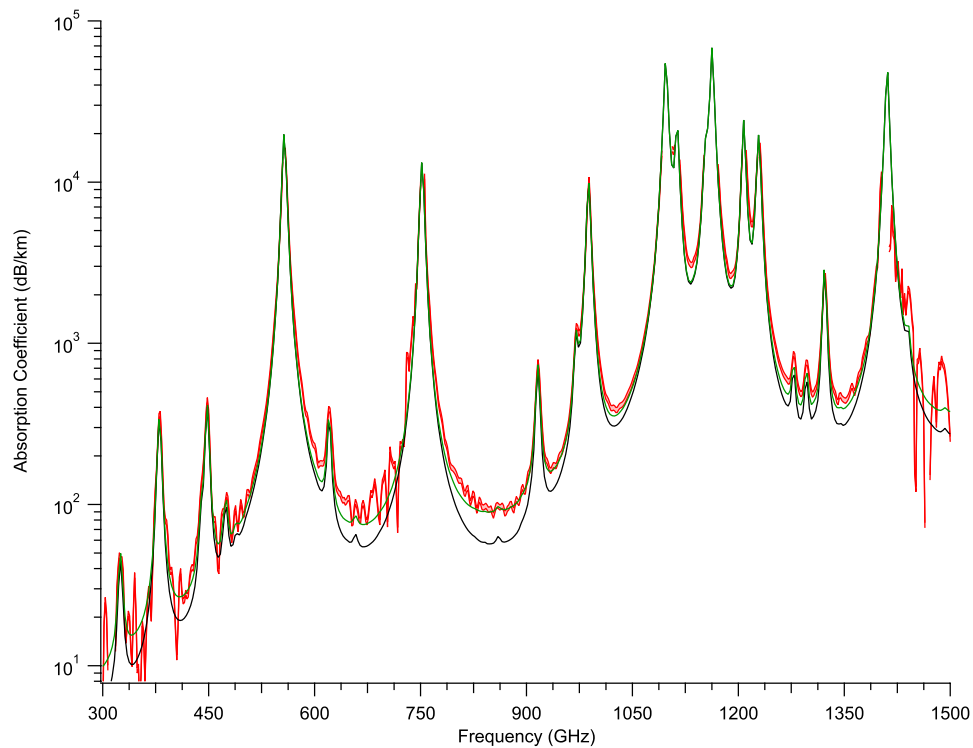


Figure 7. A comparison of the experimental absorption coefficient (red) and the calculated absorption coefficient both with (green) and without (black) a continuum contribution. All plots are for 10.05Torr of water vapor and 750.95Torr of air

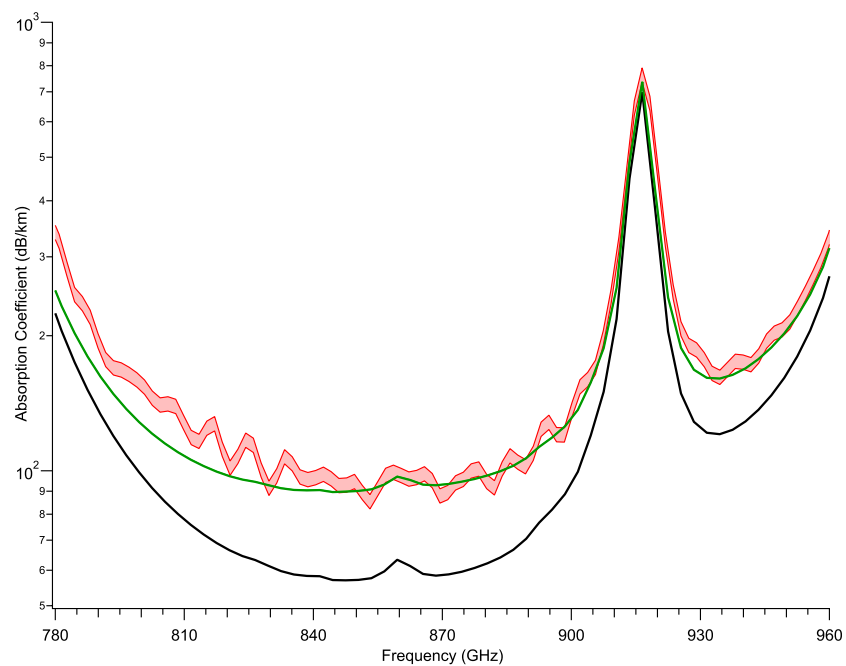


Figure 8. The same plots as Figure 7 zoomed in on a window region of the spectra.

The calculation process outlined in Section 3 was also used to model a broad range of experimental absorption data found in the literature, the results of which can be seen in Figure 9. The calculations provide good agreement with the experimental data collected using four different collection techniques; cavity Q measurements,^{9,20,22-25} Time Domain Spectroscopy,²⁶ direct attenuation measurements²⁰ and FTS measurements from the present study. The calculations are also able to accurately model a wide range of conditions including self-broadening at low pressures, and foreign gas broadening at both low and high water vapor pressures for temperatures ranging from 296-376K. The calculations for this figure used the continuum parameter set from Kuhn et al. The experimental data displayed in the figure were taken at varying temperatures. The present study was not able to determine the temperature dependence of the continuum, which is necessary to accurately model the wide range of data in the figure. Another important consideration when comparing experimental data obtained using different measurement techniques is that each technique will have a different instrumentation distortion on the spectra. Therefore instrumentation distortion must be taken into account when comparing two experimental datasets or an experimental with a calculated dataset. These considerations were taken into account in Figure 9. When applied correctly these calculations can be very useful in setting up an experiment or designing a device that will incorporate the propagation of terahertz radiation through the open atmosphere. Given some range of operating conditions the calculations can establish how much signal can be expected at the receiver after travelling some know distance. This knowledge can aid in the choice of the source and receiver used as well as setting realistic propagation distances.

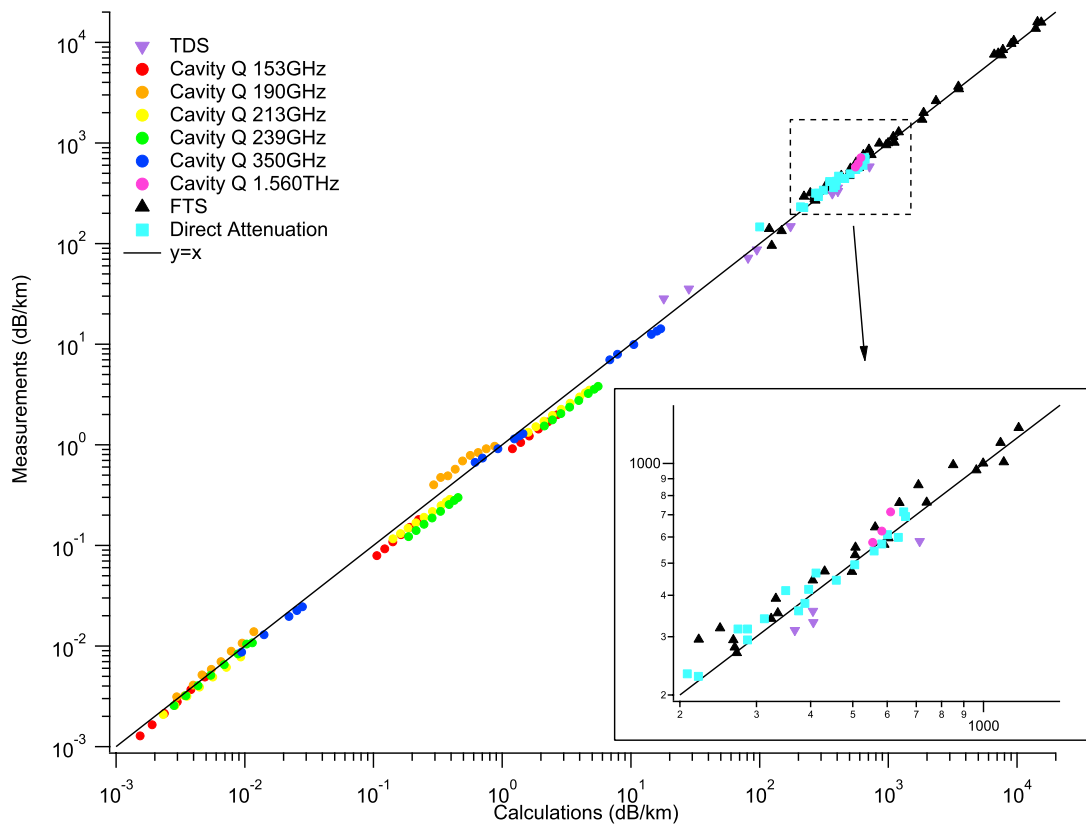


Figure 9. Correlation Plot of experimental data from the literature and the absorption coefficient calculations.

Figure 10 shows a comparison of calculated absorption coefficient values for 1Torr of water vapor and 750Torr of nitrogen for 296K at two different frequencies. The spectra have a continuum absorption contribution and have the same calculation parameters except for the high frequency limit. As can be seen in the figure, the absorption coefficient increase with the increase of the high frequency limit. This is expected as a larger high frequency limit means the inclusion of more absorption lines each contributing to the absorption coefficient at every frequency. However, the effect reaches saturation when the lines are sufficiently far from the studied frequency. The frequency difference

required to be sufficiently far may not be a constant or even a proportional value, but is influenced by the magnitude of the absorption coefficient at the studied frequency. The percent change in the absorption coefficient for a given change in the high frequency limit is larger when the magnitude of the absorption coefficient is larger. The reference value for the 846GHz data is $1.8977 \times 10^{-3} \text{m}^{-1}$ and for the 1.56THz data it is $1.4971 \times 10^{-2} \text{m}^{-1}$. The percent change in the absorption coefficient is smaller for the larger of the two reference values. This is because the additional absorption provided by the additional lines is on the same order of magnitude for both frequencies. Therefore a smaller reference value will yield a larger percent change. Since frequencies below 1THz tend to have smaller absorption coefficient values, the choice of the high frequency limit influences the calculations more at these frequencies. A calculation to 3.56THz is sufficient to reach the saturation effect at 1.56THz, while for a measurement at 846GHz a calculation to 4.46THz is required to reach saturation.

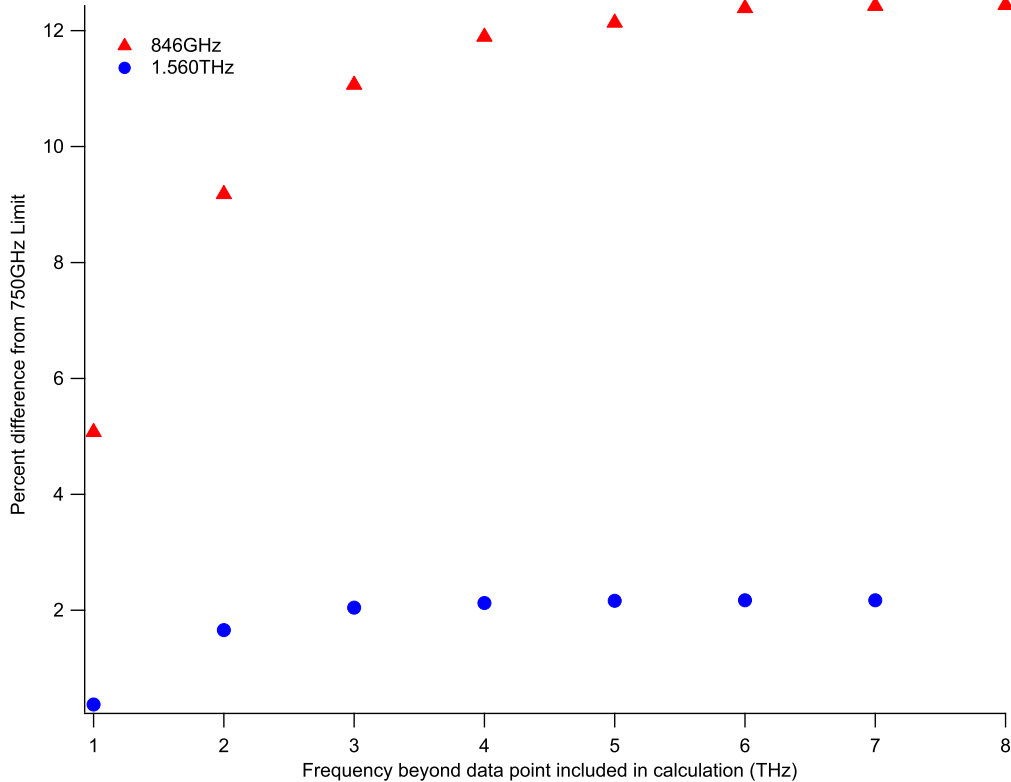


Figure 10. Comparison of calculated absorption coefficients with different high frequency limits. The reference absorption coefficient value for the percent difference calculation is from the calculation with the high frequency limit 750GHz beyond the specified frequency.

6 ABSORPTION COEFFICIENT PREDICTIONS

The calculation routine described in Section 3 was used to create predictions of the absorption coefficient of atmospheric air for varying relative humidity levels. Datasets were created for 0-3THz at 296K with 10-90% relative humidity in 10% increments. The calculations contain a continuum absorption contribution calculated using the parameter set from the present study and do not account for any instrumentation distortion. Figure 11 shows four such plots for 10, 30, 50 and 90% relative humidity. Marked in the figure are 16 atmospheric windows where the absorption coefficient has been determined and displayed in Table 1.

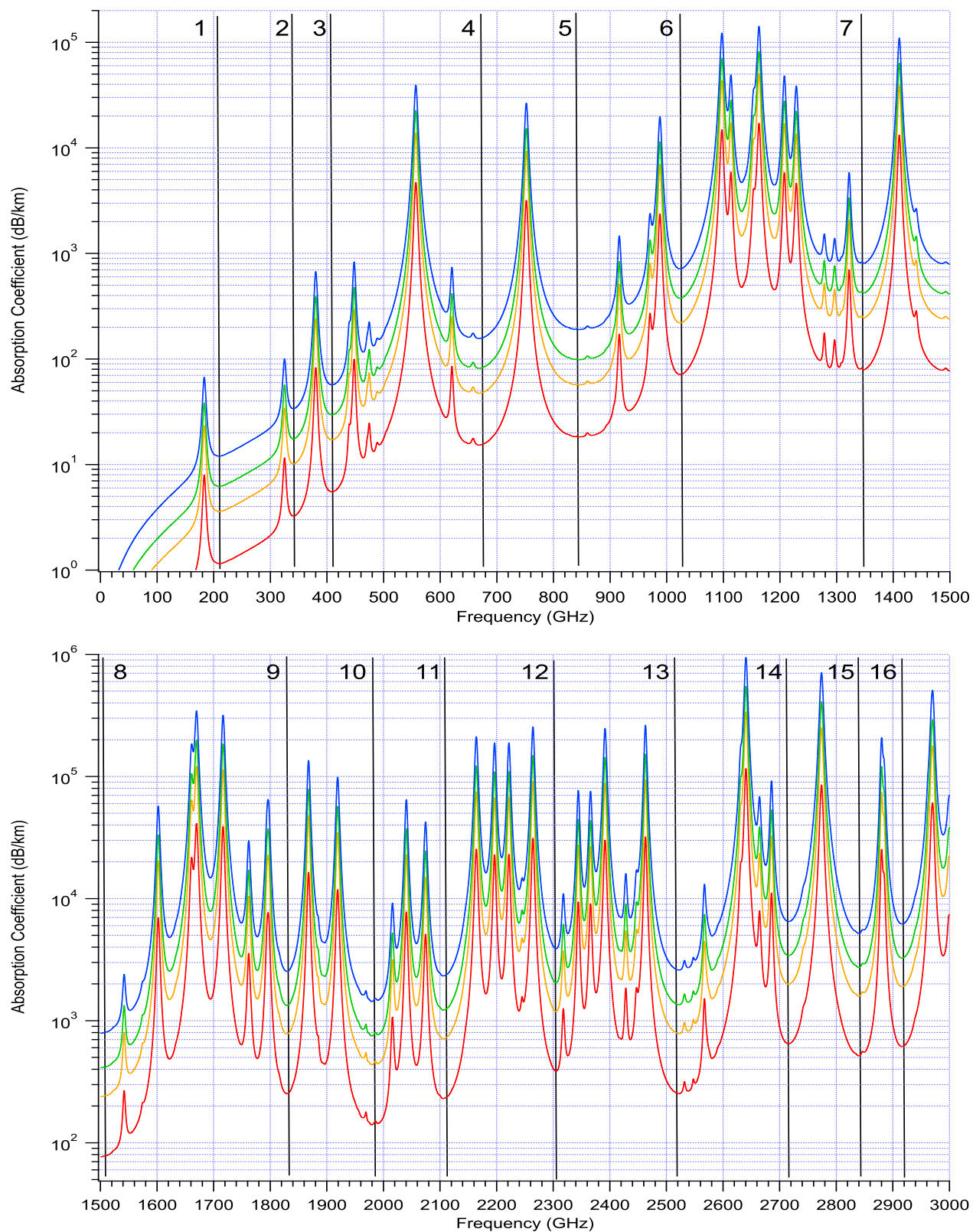


Figure 11. Calculated absorption coefficient values of water vapor at 296K for 10, 30, 50, and 90 percent relative humidity.

Table 1. A list of the calculated absorption coefficient values in dB/km of atmospheric air of varying relative humidity at 296K for the windows identified in Figure 11.

Frequency (GHz)	10%	20%	30%	40%	50%	60%	70%	80%	90%
215.543	1.170	2.370	3.630	4.940	6.290	7.690	9.140	10.60	12.20
340.630	3.250	6.610	10.10	13.80	17.50	21.40	25.40	29.50	33.80
408.657	5.520	11.20	17.20	23.30	29.60	36.10	42.90	49.80	57.00
668.519	15.30	31.00	47.40	64.30	81.70	99.50	118.0	137.0	156.0
845.159	18.20	37.10	56.80	77.20	98.30	120.0	143.0	166.0	190.0
1023.632	71.30	144.0	220.0	297.0	377.0	458.0	542.0	628.0	716.0
1348.493	79.30	161.0	245.0	333.0	422.0	514.0	609.0	707.0	807.0
1501.388	76.90	156.0	238.0	324.0	411.0	502.0	595.0	691.0	790.0
1829.587	252.0	511.0	778.0	1050	1330	1620	1920	2220	2540
1979.331	140.0	285.0	435.0	589.0	749.0	913.0	1080	1260	1440
2105.282	230.0	467.0	711.0	963.0	1220	1490	1760	2040	2330
2304.914	385.0	781.0	1190	1610	2040	2480	2940	3410	3890
2522.282	253.0	513.0	784.0	1060	1350	1650	1960	2270	2600
2715.789	648.0	1310	1990	2700	3420	4150	4910	5690	6480
2839.913	515.0	1040	1590	2150	2730	3320	3930	4550	5190
2916.306	615.0	1250	1900	2570	3260	3970	4690	5440	6200

7. Conclusions

Presented in this paper are broadband absorption measurements of air with varying levels of relative humidity for the 0.300-1.500THz frequency regime. FTS measurements of transmission spectra were recorded over multiple path lengths and used to determine the absorption coefficient as a function of frequency. These experimental absorption spectra along with calculated absorption spectra were used to calculate the air-broadened continuum coefficient to be $1.158 \times 10^{-18} \text{ m}^{-1} / (\text{Torr}^2 \text{ MHz}^2)$. This value is within the scatter of values previously reported in the literature. The calculation routine was also used to model experimental water vapor absorption data from other authors. The calculations provide good agreement to the data for four measurement techniques with a wide range of experimental parameters over 8 orders of magnitude in the absorption coefficient. This calculation routine can be used as an accurate predictive tool for atmospheric absorption of terahertz radiation when the continuum contribution is accounted for. It was shown that instrumentation distortion must be accounted for before a comparison of data can be made between different collection techniques. If the continuum is not included, the discrepancy between the calculations and experiment could be as large as 90dB over a one kilometer path length.

References

- [1] Payne, V. H., Delamere, J. S., Cady-Pereira, K. E., Gamache, R. R., Moncet, J. L., Mlawer, E. J. and Clough, S. A., "Air-Broadened Half-Widths of the 22- and 183-GHz Water-Vapor Lines," *IEEE Trans. Geosci. Remote Sens.* 46(11), 3601-3617 (2008).
- [2] Gamache, R. R. and Laraia, A. L., "N₂- O₂-, and air-broadened half-widths, their temperature dependence, and line shifts for the rotational band of H₂¹⁶O," *J. Mol. Spectrosc.* 257(2), 116-127 (2009).
- [3] Ma, Q., Tipping, R. H. and Gamache, R. R., "Uncertainties associated with theoretically calculated N₂-broadened half-widths of H₂O lines," *Mol. Phys.* 108(17), 2225-2252 (2010).
- [4] Ma, Q. and Tipping, R. H., "Water vapor continuum in the millimeter spectral region," *J. Chem. Phys.* 93(9), 6127-6139 (1990).
- [5] Liebe, H. J., "MPM-An Atmospheric Millimeter-Wave Propagation Model," *Int. J. Infrared Milli Waves* 10(6), 631-650 (1989).
- [6] Liebe, H. J., Hufford, G. A. and Cotton, M. G., "Propagation Modeling Of Moist Air and Suspended Water/Ice Particles at Frequencies Below 1000 GHz," *Proceedings of the AGARD 52nd Specialists Meeting of the Electromagnetic Wave Propagation Panel, Palma de Mallorca, Spain, 1993.*
- [7] Pardo, J. R., Cernicharo, J. and Serabyn, E., "Atmospheric Transmission at Microwaves (ATM): An Improved Model for Millimeter/Submillimeter Applications," *IEEE T Antenn. Propag.* 49(12), 1683-1694 (2001).
- [8] Rosenkranz, P. W., "Water vapor microwave continuum absorption: A comparison of measurements and models," *Rad. Sci.* 33(4), 919-928 (1998).
- [9] Kuhn, T., Bauer, A., Godon, M., Buhler, S. and Kunzi, K., "Water vapor continuum: absorption measurements at 350GHz and model calculations," *JQSRT* 74(5), 545-562 (2002).
- [10] Liebe, H. J. and Layton, D. H., "Millimeter-wave properties of the atmosphere: laboratory studies and propagation modeling," *NTIA Rep. 87-224, Natl. Telecommun. And Inf. Admin., Boulder, Co, 1987.*
- [11] Pardo, J. R., Serabyn, E. and Cernicharo, J., "Submillimeter atmospheric transmission measurements on Mauna Kea during extremely dry El Nino conditions: implications for broadband opacity contributions," *JQSRT* 68(4), 419-433 (2001).
- [12] Podobedov, V. B., Plusquellic, D. F. and Fraser, G. T., "Investigation of the water-vapor continuum in the THz region using a multipass cell," *JQSRT* 91(3), 287-295 (2005).
- [13] Podobedov, V. B., Plusquellic, D. F., Siegrist, K. E., Fraser, G. T., Ma, Q. and Tipping, R. H., "New Measurements of the water vapor continuum in the region from 0.3 to 2.7THz," *JQSRT* 109(3), 458-467 (2008).
- [14] Podobedov, V. B., Plusquellic, D. F., Siegrist, K. M., Fraser, G. T., Ma, Q. and Tipping, R. H., "Continuum and magnetic dipole absorption of the water vapor-oxygen mixtures from 0.3 to 3.6 THz," *J. Mol. Spec.* 251(1-2), 203-209 (2008).
- [15] Burch, D. E., "Absorption of Infrared Radiant Energy by CO₂ and H₂O. III. Absorption by H₂O between 0.5 and 36 cm⁻¹ (278 μ-2 cm)," *J. Opt. Soc. Am.* 58(10), 1383-1394 (1968).
- [16] Serabyn, E., Weisstein, E. W., Lis, D. C. and Pardo, J. R., "Submillimeter Fourier-transform spectrometer measurements of atmospheric opacity above Mauna Kea," *Appl. Opt.* 37(12), 2185-2198 (1998).
- [17] Matsuo, H., Sakamoto, A. and Matsushita, S., "FTS Measurements of Submillimeter-Wave Atmospheric Opacity at Pampa la Bola," *Publ. Astron. Soc. Japan* 50, 359-366 (1998).

- [18] Paine, S., Blundell, R., Papa, D. C., Barrett, J. W. and Radford, S. J. E., "A Fourier Transform Spectrometer for Measurement of Atmospheric Transmission at Submillimeter Wavelengths," Publ. Astron. Soc. Pacific 112, 108-118 (2000).
- [19] Rothman, L. S., Gordon, I. E., Barbe, A., Chris Benner, D., Bernath, P. F., Birk, M., Boudon, V., Brown, L. R., Campargue, A., Champion, J. P., Chance, K., Coudert, L. H., Dana, V., Devi, V. M., Fally, S., Flaud, J. M., Gamache, R. R., Goldman, A., Jacquemart, D., Kleiner, I., Lacome, N., Lafferty, W. J., Mandin, J. Y., Massie, S. T., Mikhailenko, S. N., Miller, C. E., Moazzen-Ahmadi, N., Naumenko, O. V., Nikitin, A. V., Orphal, J., Perevalov, V. I., Perrin, A., Predoi-Cross, A., Rinsland, C. P., Rotger, M., Simeckova, M., Smith, M. A. H., Sung, K., Tashkun, S. A., Tennyson, J., Toth, R. A., Vandaele, A. C. and Vander Auwera, J., "The HITRAN 2008 molecular spectroscopic database," JQSRT 110(9-10), 533-572 (2009).
- [20] Slocum, D. M., Slingerland, E. J., Giles, R. H. and Goyette, T. M., "Atmospheric Absorption of Terahertz Radiation and Water Vapor Continuum Effects," JQSRT, accepted 4/21/13.
- [21] Van Vleck, J. H. and Weisskopf, V. F., "On the Shape of Collision-Broadened Lines," Rev. Mod. Phys. 17 (2-3), 227-236 (1945).
- [22] Bauer, A. and Godon, M., "Temperature Dependence of Water-Vapor Absorption in Linewings at 190GHz," JQSRT 46(3), 211-220 (1990).
- [23] Godon, M., Carlier, J. and Bauer, A., "Laboratory Studies of Water Vapor Absorption in the Atmospheric Window at 213GHz," JQSRT 47(4), 275-285 (1991).
- [24] Bauer, A., Godon, M., Carlier, J., Ma, Q. and Tipping, R. H., "Absorption by H₂O and H₂O-N₂ Mixtures at 153GHz," JQSRT 50(5), 463-475 (1993).
- [25] Bauer, A., Godon, M., Carlier, J. and Ma, Q., "Water Vapor Absorption in the Atmospheric Window at 239GHz," JQSRT 53(4), 411-423 (1994).
- [26] Yang, Y., Shutler, A. and Grischkowsky, D., "Measurement of the transmission of the atmosphere from 0.2 to 2THz," Opt. Express 19(9), 8830-8838 (2011).